

SEISMIC HAZARD IN THE PANNONIAN REGION

László Tóth^{1,3}, Erzsébet Györi², Péter Mónus^{1,3}, Tibor Zsíros^{1,3}

1: *Seismological Observatory, Hungarian Academy of Sciences, Budapest, Hungary*
toth@georisk.hu

2: *Research Group of Geophysics and Environmental Physics of HAS, Budapest, Hungary*

3: *GeoRisk Earthquake Research Institute, Budapest, Hungary*

ABSTRACT

Seismic hazard for single sites and hazard maps for the whole Pannonian region (44.0-50.0N; 13.0-28.0E) have been calculated. The hazard assessment was carried out using a probabilistic approach by incorporating a wide range of parameter values and viable interpretations that were consistent with the data. Alternative interpretations were described by branches of a logic tree. Each branch was weighted according to the ability of that interpretation to explain the available data. The resulting seismic hazard map describes expected shaking with a 475-year return period in terms of peak ground acceleration. Furthermore, some important contributors to seismic risk are highlighted, and a liquefaction hazard map is presented for the territory of Hungary.

Keywords: seismicity, seismic hazard, Pannonian Basin

INTRODUCTION

The Pannonian region is situated between the Mediterranean area, which is one of the most seismically active regions in the world, and the East European platform, which can be treated as nearly aseismic. Deformation in the Pannonian basin system is ongoing (Bada et al. 1998, Horváth and Cloetingh 1996). One of the most direct pieces of evidence for the continuing deformation, in addition to GPS geodetic data (Grenerczy et al. 2002), is current seismic activity (Bada et al. 1999, Gerner et al. 1999).

In the following paper, we give a brief review of seismic hazard methodology, present the latest seismic hazard map of the region and highlight some chief factors (e.g., site effect, liquefaction) contributing to seismic risk.

SEISMICITY SUMMARY

Seismic activity in the Pannonian region can be characterized as moderate, with significant variations in different tectonic domains. The highest seismicity rate is observed in the Vrancea region in the southeast Carpathians, where strong earthquakes occur quite frequently. Within the last decades, three events were detected with magnitudes larger than 6.5 (1977: M7.2; 1986: M7.0; 1990: M6.7), while magnitude 5.0 earthquakes occur on an almost yearly basis.

In the less active Pannonian basin area (about 200,000 km²), the return period of magnitude 6 earthquakes is about 100 years while magnitude 5 events occur every 20 years on average. Based on the results of high sensitivity monitoring in the last decade (Tóth et al. 2004), the average number of magnitude 3 earthquakes is 4 per year while that of magnitude 2 events is about 30 per year.

Distribution of focal depths suggests three depth domains. Shallow focal depths within the top 20 km of the earth's crust occur almost exclusively through the whole Pannonian region except the Vrancea zone. In the Pannonian basin, the majority of events occur between 6 and 15 km below ground level. Earthquakes of the Vrancea region are characterized by intermediate depths. Strong earthquakes occur between either 70-110 km or 125-160 km depth domains within an almost vertical column. Deeper and shallower events also have been recorded but only with small magnitudes.

Inferred from focal mechanism solutions (Tóth et al., 2002), strike-slip and thrust faulting occurs almost exclusively through the Southern Alps and the Dinarides. The maximum horizontal stress direction clearly shows N-S and NNE-SSW compression that can be explained by the collision of Adria with Europe.

Moderately active seismicity is observed in the Eastern Alps and the western Carpathians. Focal mechanism solutions are available mostly from the Vienna Basin area, documenting exclusively strike-slip mechanisms. NNW-SSE and N-S directions of the largest horizontal stresses are the most frequent, but NE-SW directions are occasionally encountered.

In the Pannonian Basin, the picture shown by the focal mechanism solutions is more diverse, however thrust and strike-slip faulting seems to be dominant. NNE-SSW and NE-SW directions of maximum horizontal stresses prevail, highlighting significant differences from Western Europe, where the dominant stress direction is perpendicular to that. The very few fault-plane solutions available from the area of eastern and southern Carpathians indicate thrust faulting and E-W dominant stresses. Most events in the Vrancea area are compressional and occur at intermediate depths. Fault-plane solutions of instrumentally recorded large earthquakes show remarkably similar

characteristics. They typically strike SW-NE and dip to the NW. The maximum horizontal stress characteristically trends NW-SE and in fewer cases E-W.

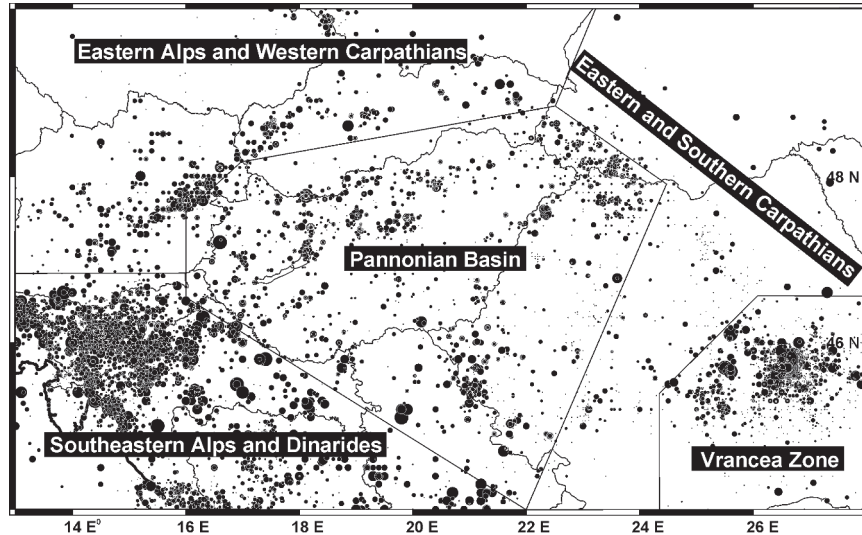


Figure 1. Seismicity of the Pannonian region (44.0-50.0N; 13.0-28.0E). The earthquake database contains more than 20,000 historical and instrumentally recorded events from 456 AD until 2002.

SEISMIC HAZARD METHODOLOGY APPLIED

Seismic hazard is the probabilistic measure of ground shaking associated with the recurrence of earthquakes as originally defined by Cornell (1968). Seismic hazard shows the level of chosen ground motion that likely will not be exceeded during a specified time interval. Hazard assessment for civil use commonly specifies a 90% probability of non-exceedance of some ground motion parameter (most often ground acceleration) for an exposure time of 50 years, corresponding to a return period of 475 years. For nuclear power plants and other installations posing higher environmental risk, it is common practice to use much lower probability events on the order of 10^{-4} to 10^{-6} /year.

The methodology used to assess seismic hazard and the associated uncertainty at nuclear and non-nuclear fields must provide technically sound results and should: be experience-based, be data-driven, incorporate proper treatment of uncertainties, be flexible and facilitate sensitivity analysis.

Six essential steps are involved in the assessment of seismic hazard:

Step 1: Evaluation of seismic sources.

Estimate the geometries and spatial distribution of potential sources of future seismic activity in the region. Characterize the assumed uncertainty in the spatial description of each source.

Step 2: Characterization of seismic sources.

For each seismic source, describe the distribution of occurrence rates of future earthquakes as a function of magnitude. Estimate the maximum magnitude for each source. Characterize the uncertainty in recurrence relations and in maximum magnitude.

Step 3: Ground motion attenuation.

Evaluate or estimate relations that express how the amplitudes of selected ground-motion parameters vary with earthquake magnitude and distance for the region. Characterize the uncertainty in these ground-motion attenuation relations.

Step 4: Mathematical model to calculate seismic hazard.

Calculate the seismic hazard for each combination of inputs (determined in steps 1-3) and integrate the results. Plot a curve expressing the annual probability that a given value of ground motion will be exceeded. Carry out the integration for all combinations of inputs to incorporate the variability of input estimates.

Step 5: Presentation of the hazard results.

Express the results of step 4 as a distribution of seismic hazard curves that can be represented by a mean curve and curves representing particular percentiles of the distribution.

Step 6: Site effect, secondary seismic effects

Calculate the influence of the local geological setting on the ground motion.

DATABASE

The first and most important component of a probabilistic seismic hazard study is the compilation of the geological, geophysical and geotechnical data on regional (1:500,000), near-regional (1:50,000), site vicinity (1:5,000) and site area (1:500) scales. Seismological databases are developed on different time scale zooming on different event recurrence rates such as paleo-earthquakes ($<10^{-3}/\text{yr}$), historical earthquakes ($10^{-3}-10^{-2}/\text{yr}$), instrumental earthquake data ($10^{-2}-10^{-1}/\text{yr}$) and site-specific instrumental data or local seismic monitoring ($>10^{-1}/\text{yr}$).

The geology and tectonic evolution of the Pannonian region has been studied intensively over recent decades. The development of the Carpathian mountain belt and the Pannonian basin has been attributed to the collision between the Eurasian Plate and the African Plate between the Paleocene and Middle-Late Miocene (e.g., Horváth, 1988; Csontos et al., 2002; Fodor et al., 1999).

The comprehensive earthquake catalogue of the Pannonian region (44.0-50.0 N latitude and 13.0-28.0 E longitude) contains more than 20,000 events ranging from 456 A.D. to the present. The preparation of the earthquake catalogue is documented in detail in Zsíros (2000), Tóth et al. (2002) and Zsíros (2003a and 2003b).

Magnitude

The earthquake catalogue of the Pannonian region goes far back to pre-instrumental time. However, for historical earthquakes the only source of information is macro seismic observation. It seems rational to suppose that there is some relation between magnitude, epicentral intensity and depth. Many authors (eg. Csomor and Kiss, 1959; Karnik, 1968) suppose that magnitude depends on epicentral intensity and focal depth according to the relation:

$$M_M = a I_0 + b \log h + c$$

where M_M is the macroseismic magnitude, I_0 the epicentral intensity, h the focal depth in km; and a , b , c are constant parameters.

Table 1 shows the best-fit constants in the above equation for shallow Pannonian-region earthquakes, and for intermediate-depth events in the Vrancea region.

Table 1. Value and uncertainty of a , b and c in $M_M = a I_0 + b \log h + c$, as well as the magnitude and intensity intervals and the number of events N .

Area	a	b	c
for the Pannonian region $1 \leq h \leq 65$ $\text{III} \leq I_0 \leq \text{X}$ $0.6 \leq M_M \leq 6.2$ $N = 514$	0.68 ± 0.02	0.96 ± 0.07	-0.91 ± 0.10
for the Vrancea region $1 \leq h \leq 200$ $\text{II} \leq I_0 \leq \text{IX}$ $2.4 \leq M_M \leq 7.3$ $N = 130$	0.52 ± 0.02	0.55 ± 0.11	1.18 ± 0.20

The best-fit relation for shallow Pannonian-region earthquakes using 12.6 km average focal depth gives: $M_M = 0.68 I_0 + 0.15$.

For intermediate-depth seismicity in the Vrancea region, using 92.5 km average focal depth: $M_M = 0.52 I_0 + 2.27$.

A simple linear regression between measured surface-wave magnitude (M_S) and epicentral intensity (I_0) for the whole catalogue of events where both M_S and I_0 exist, gives: $M_S = 0.74 I_0 - 0.28$. The macroseismic and surface-wave magnitude values estimated from intensity are generally quite similar (Tóth et al., 2002). Table 2 shows the empirical relations between different magnitude scales used in the earthquake catalogue.

Table 2. Value and uncertainty of a and b in the equation of $M_X = a M_Y + b$ as well as the magnitude intervals and the number of events N .

	M_M	M_B	M_L	M_D
$M_S =$	$a = 1.03 \pm 0.02$ $b = -0.20 \pm 0.10$ $2.0 \leq M_S \leq 7.0$ $2.0 \leq M_M \leq 6.8$ $N = 186$	$a = 0.97 \pm 0.05$ $b = 0.04 \pm 0.24$ $2.5 \leq M_S \leq 7.0$ $2.1 \leq M_B \leq 6.4$ $N = 127$	$a = 0.86 \pm 0.06$ $b = 0.57 \pm 0.27$ $2.0 \leq M_S \leq 7.0$ $2.0 \leq M_L \leq 6.6$ $N = 97$	$a = 1.21 \pm 0.11$ $b = -1.23 \pm 0.52$ $2.3 \leq M_S \leq 6.9$ $2.8 \leq M_D \leq 6.5$ $N = 27$
$M_B =$			$a = 0.59 \pm 0.55$ $b = 1.75 \pm 0.22$ $2.6 \leq M_B \leq 6.4$ $2.1 \leq M_L \leq 6.6$ $N = 259$	$a = 0.90 \pm 0.08$ $b = 0.20 \pm 0.32$ $2.6 \leq M_B \leq 6.3$ $3.2 \leq M_D \leq 6.5$ $N = 160$
$M_L =$				$a = 1.14 \pm 0.02$ $b = -0.69 \pm 0.06$ $0.8 \leq M_L \leq 5.5$ $1.4 \leq M_D \leq 5.6$ $N = 894$

Earthquake recurrence

Seismicity in the Pannonian area is a typical example of distributed seismicity. Due to inaccurate seismic and geological information, most earthquakes cannot be assigned to specific tectonic structures: i.e., the present seismotectonic knowledge of the area does not allow us to ascertain which fault produced which earthquake. This is particularly true for events below magnitude 4. For large historical earthquakes, the difficulty mostly comes from inaccurate hypocenter information. In areas where underlying faults are unknown, the current practice is to represent the temporal occurrence of earthquakes as a Poisson process. For this purpose, all foreshocks and aftershocks should be removed from the earthquake catalogue, and the

completeness of the catalogue should be assessed. In a complete catalogue, all earthquakes above a lower bound magnitude – the threshold magnitude M_0 – are assumed to be included.

For identifying main shocks, space and time filters should be applied. Dieterich (1994) proposed that the aftershock duration T generally increases with the inferred recurrence time of the main shock T_r such that $T \approx T_r/20$. Stein and Newman (2004) put forward the possibility of much longer aftershock duration for low seismicity intraplate settings, especially for the New Madrid area. This possibility could be explained by higher earthquake stress drops and larger normal stresses on intraplate faults and would have major consequences for seismic hazard of low seismicity areas.

Based on empirical considerations and on our professional judgment to some extent, we used a magnitude-dependent space and time filter to identify main shocks in the catalogue as detailed by Table 3.

Table 3. Space and time windows used for filtering out the aftershocks and foreshocks from the catalogue. In the vicinity of radius R of the magnitude M main earthquake, all shocks with $M' < M$ are regarded as aftershocks or foreshocks if their origin time difference is less than T or T' respectively

Magnitude	R (km)	T (day)	T' (day)
$M_M \leq 1.8$	5	1	1
$1.9 \leq M_M \leq 2.7$	10	2	1
$2.8 \leq M_M \leq 3.3$	15	5	1
$3.4 \leq M_M \leq 4.0$	20	30	2
$4.1 \leq M_M \leq 4.7$	25	130	4
$4.8 \leq M_M \leq 5.4$	30	260	10
$5.5 \leq M_M \leq 6.1$	35	650	15
$6.2 \leq M_M$	40	850	30

A simple comprehensiveness test based on “magnitude recurrence fit” shows that our catalogue is complete since 1500 for magnitude $M_0 \geq 6.4$, since 1600 for magnitude $M_0 \geq 5.8$, since 1700 for magnitude $M_0 \geq 5.3$, since 1800 for magnitude $M_0 \geq 4.7$, since 1850 for magnitude $M_0 \geq 4.2$, and since 1880 for magnitude $M_0 \geq 3.5$ for the whole Pannonian region (Table 4).

The probability of earthquake occurrence as a function of magnitude is generally represented by an exponential distribution, as proposed by Gutenberg and Richter (1944): $\log N = a - bM$, where N is the annual number of earthquakes with magnitude equal or greater than M . From the whole Pannonian region dataset, we find that $a = 5.27 \pm 0.11$ and $b = 1.04 \pm 0.02$ in the $3.5 \leq M_M \leq 7.3$ magnitude range.

Table 4. Completeness test results for the Pannonian region earthquake catalogue

The catalogue is complete	for magnitude
since 1500	$M_0 \geq 6.4$
since 1600	$M_0 \geq 5.8$
since 1700	$M_0 \geq 5.3$
since 1800	$M_0 \geq 4.7$
since 1850	$M_0 \geq 4.2$
since 1880	$M_0 \geq 3.5$

EVALUATION AND CHARACTERIZATION OF SEISMIC SOURCES

In seismic source modeling, a thorough analysis of the main tectonic structures and their correlation with seismicity is the basis for the definition of the source zones. Three source zone models (M1, M2 and M3) were defined with 20, 25, and 15 zones, respectively.

Due to the diffuse seismicity of the whole region, specific faults cannot be identified. We deal here with polygons within which future earthquakes may occur (Figure 2).

An important parameter for source zone characterization is the maximum magnitude value. M_{\max} values were assigned only on a seismological basis; seismotectonic or geological evidences were not considered in this respect. The one-step-beyond technique (Slejko et al., 1998) was applied where the number of earthquakes was large enough: the rates were fitted by the Gutenberg-Richter relationship, and the extrapolated rate for a magnitude greater than the maximum observed value by 0.5 magnitude value. In addition, variations were added to handle epistemic uncertainty (Table 5).

The present-day crustal velocity field derived from GPS measurements (Grenerczy et al., 2002) shows that the largest velocities (1.5-2 mm/yr northward) in the Pannonian region can be found in the SW, located in the Alpine-Adriatic collision zone. Inside the Pannonian basin, the typical velocity is about 1.0-1.5 mm/yr eastward.

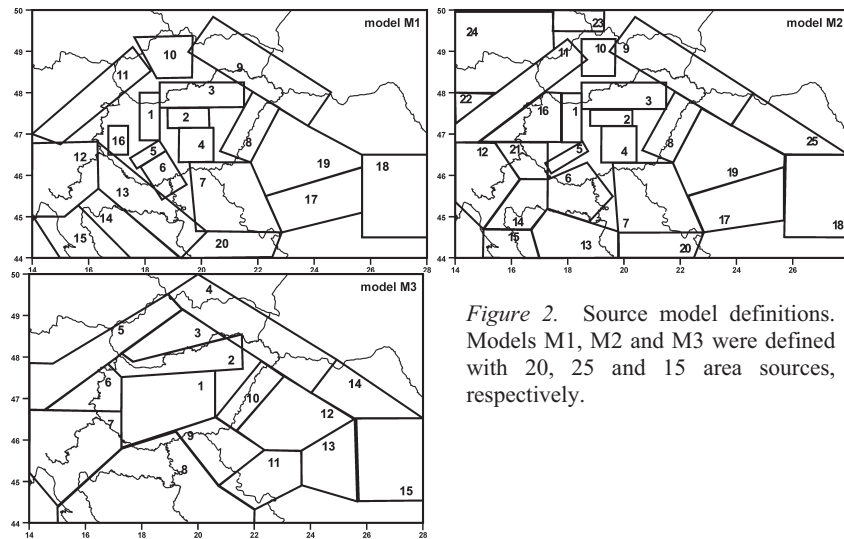


Figure 2. Source model definitions. Models M1, M2 and M3 were defined with 20, 25 and 15 area sources, respectively.

Table 5. Source models M1, M2, M3 and different M_{max} values used in the hazard computations for source zones (see Figure 2 for the definition of the polygons)

Zone #	Source model M1			Source model M2			Source model M3		
	M_{max}^1	M_{max}^2	M_{max}^3	M_{max}^1	M_{max}^2	M_{max}^3	M_{max}^1	M_{max}^2	M_{max}^3
1	6.2	6.4	6.0	6.2	6.4	6.0	6.0	6.2	5.8
2	6.0	6.2	5.8	6.0	6.2	5.8	6.2	6.4	5.8
3	5.8	6.0	5.5	5.8	6.0	5.5	5.8	6.0	5.6
4	6.0	6.2	5.8	6.0	6.2	5.8	5.8	6.0	5.6
5	5.4	5.8	5.0	5.4	5.8	5.0	6.2	6.4	6.0
6	5.8	6.0	5.6	6.0	6.2	5.8	5.4	5.6	5.2
7	6.0	6.2	5.8	6.0	6.2	5.8	6.5	6.7	6.3
8	6.2	6.4	6.0	6.2	6.4	6.0	6.2	6.5	6.0
9	5.8	6.0	5.4	5.8	6.0	5.4	6.0	6.2	5.8
10	5.8	6.0	5.6	5.8	6.0	5.6	6.2	6.4	6.0
11	6.2	6.4	6.0	6.2	6.4	6.0	6.0	6.2	5.8
12	6.5	6.7	6.3	6.5	6.7	6.3	5.6	6.0	5.2
13	6.2	6.4	6.0	6.2	6.4	6.0	6.5	6.7	6.4
14	6.2	6.4	6.0	6.2	6.4	6.0	5.8	6.0	5.6
15s	6.2	6.4	6.0	6.0	6.2	5.8	6.0	6.2	5.8
15d							7.5	7.7	7.3
16	5.4	5.6	5.2	5.4	5.6	5.2			
17	6.5	6.7	6.4	6.5	6.7	6.4			
18s	6.0	6.2	5.8	6.0	6.2	5.8			
18d	7.5	7.7	7.3	7.5	7.7	7.3			
19	5.6	6.0	5.2	5.6	6.0	5.2			
20	6.2	6.4	6.0	6.2	6.4	6.0			
21				6.0	6.2	5.8			
22				5.8	6.0	5.6			
23				5.6	5.8	5.4			
24				5.8	5.8	5.2			
25				5.8	6.0	5.6			

These values seem to be in accordance with earthquake recurrence estimated from historical and instrumental seismicity. However, Lenkey et al. (2002) suggested that seismicity in the region is mainly controlled by the different thermal conditions of the lithosphere.

GROUND MOTION ATTENUATION

Attenuation relations for the Pannonian region based on the strong motion data are practically non-existent. Based on the analysis of macroseismic effects and intensity attenuation, Zsíros (1996) concluded that the attenuation of ground motion with distance in the Pannonian basin is greater than in many similar areas with low to moderate seismicity.

For the hazard computations in this study, attenuation relations developed by Ambraseys et al. (1996), Boore et al. (1997) and Sadigh et al. (1997) were adopted with 1/2, 1/4, and 1/4 weights respectively.

MATHEMATICAL MODEL TO CALCULATE SEISMIC HAZARD

We established a logic tree including all uncertainties involved (Figure 3). Uncertainty in seismic source evaluation was represented by weighted alternative seismotectonic models; uncertainty in recurrence was characterized by probability distributions on the recurrence parameters; and uncertainty in ground motion evaluations was characterized by a set of alternative ground-motion relationships and their associated weights.

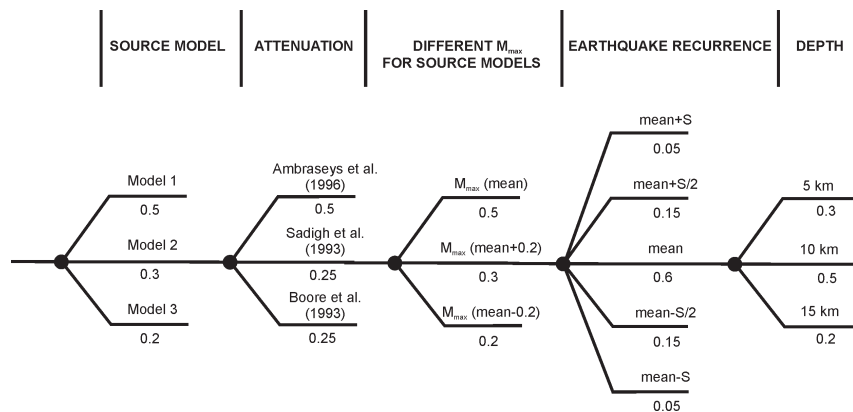


Figure 3. Simplified logic tree for the probabilistic seismic hazard computation.

SEISMIC HAZARD RESULTS

Using the methodology described above, seismic hazard curves for single sites were calculated even for very low probabilities, for example for the Paks NPP site (Figure 4). Furthermore, hazard maps for the whole Pannonian region were calculated.

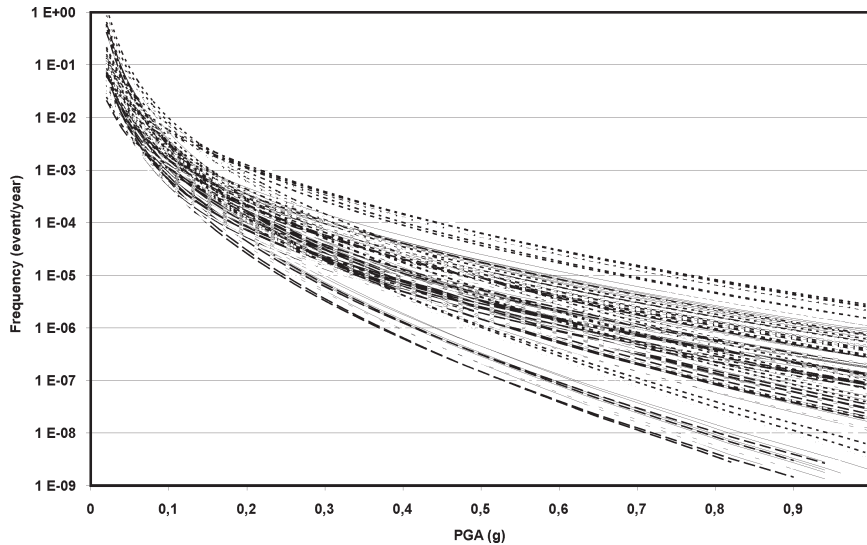


Figure 4. Seismic hazard curves for Paks NPP site along logic tree branches.

The seismic hazard map of the Pannonian region shown in Figure 5 depicts the mean PGA with a 90% probability of non-exceedance in 50 years. Not surprisingly, the highest seismic hazard values (more than $4\text{--}5\text{ m/s}^2$) are expected in the Vrancea region, corresponding to high levels of seismicity. The second highest hazard in the region is found in the Slovenia-Croatia border region (Trieste-Ljubljana-Zagreb area) with $2.0\text{--}2.5\text{ m/s}^2$ PGA. In addition, areas of relatively high seismic hazard include some other areas of moderate seismicity, such as in the Dinarides and in the Mur-Mürz valley. Most of the Pannonian basin has a relatively low seismic hazard, with less than 1 m/s^2 expected PGA, however there are some patches with greater hazard, in the range of $1\text{--}2\text{ m/s}^2$, at Komárom and northeast of Lake Balaton, east of Budapest, and the southwest portion of Hungary.

Two similar sets of maps have been released in the framework of the Global Seismic Hazard Assessment Program (GSHAP) in 1999 (Grünthal et al., 1999; Musson, 1999). It goes beyond the possibilities of the present study

to compare these maps in detail, but some fundamental similarities and a few major differences should be mentioned.



Figure 5. Seismic hazard in the Pannonian region. Expected peak ground acceleration in m/s^2 (10% probability of exceedance in 50 years, 475 year return period).

Each of the three studies employed a fairly similar method and used more-or-less identical earthquake catalogs. The largest differences are the different philosophies in evaluation and characterization of the seismic sources and the selection of suitable attenuation relationships.

Although there are similarities in general hazard levels between the different maps, hazard contours and patches of enhanced hazard are not necessarily equivalent. Obviously enough, the Vrancea region results the highest hazard values on each map. Southwest of the investigated area, the GSHAP hazard values are generally higher than our values. Our model, as well as that of Musson, spreads the historical seismicity in the Zagreb-Ljubljana-Rijeka area, whereas the GSAP map concentrates the hazard in a smaller area around Zagreb. The same outcome can be seen in some other regions, for example in the historically active Komárom region.

SITE EFFECT AND SECONDARY SEISMIC EFFECTS

Soft surface layers, strong lateral discontinuities in the immediate vicinity, or abrupt changes in topography can result in considerable amplification or alteration of earthquake-induced ground motion. These effects have to be accounted for by a calculation of the dynamic response of each site's geological setting to incoming seismic waves. The importance of this effect generally varies with frequency.

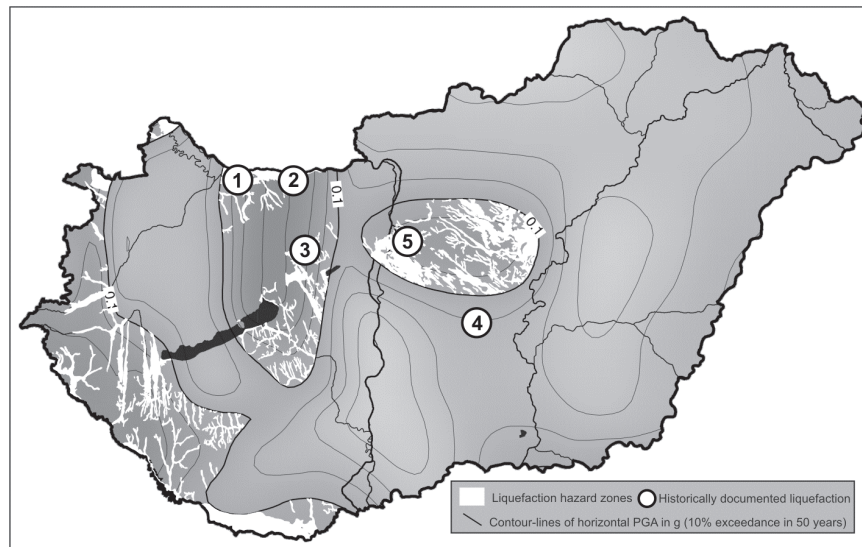


Figure 6. Liquefaction-prone areas in Hungary with 10% probability of exceedance in 50 years, 475 year return period. White dots show area of documented liquefactions after the 1 – Komárom (1763), 2 – Komárom (1783), 3 – Mór (1810), 4 – Kecskemét (1911) and 5 – Dunaharaszti (1956) earthquakes.

Large areas of the Pannonian basin are covered by young, loose sediments. One of the most serious secondary seismic effects is liquefaction ground failure. Liquefaction is defined as the temporary loss of load-bearing strength of a saturated, loose granular soil during, and for some time after an earthquake due to cyclic loading and the build-up of pore-water pressure. The likelihood of liquefaction depends primarily on the presence of water, the particle size distribution of the material, the density of the material, and the effective confining stress. Examples show that sands tend to liquefy very easily, whereas clays and gravels do not. Following the recommendations of Lew (2001) to develop liquefaction hazard maps, we have convolved the seismic hazard map shown in Figure 5 with maps of surface geology (Jámbor, 1989) and maximum ground water levels (Deseő, 1989). The map in Figure 6

shows the zones in Hungary generally prone to liquefaction. The predicted liquefaction hazard zones match fairly well with historically documented liquefaction cases, for example after the Komárom (1763, 1783), Mór (1810), Kecskemét (1911) and Dunaharaszti (1956) earthquakes.

The user communities in Hungary have responded very positively to the current seismic hazard map. The *Hungarian National Committee on Earthquake Engineering* has accepted these hazard estimates and made recommendations to their use in developing national annexes to the EUROCODE-8.

ACKNOWLEDGEMENTS

The research presented in this contribution has been supported by Paks NPP and GeoRisk Ltd. We thank Seth Stein and Francois Thouvenot for their constructive reviews and editorial assistance.

REFERENCES

- Ambraseys N., Simpson K., Boomer J. Prediction of Horizontal Response Spectra in Europe. *Earthquake Engineering and Structural Dynamics* 1996; 25: 371-400.
- Bada G., Gerner P., Cloetingh S., Horváth F. Sources of recent tectonic stress in the Pannonian region: inferences from finite element modelling. *Geophys. J. Int.* 1998; 134: 87-102.
- Bada G., Horváth F., Gerner P., Fejes I. Review of the present-day geodynamics of the Pannonian basin progress and problems. *J. Geodynamics* 1999; 27: 501-527.
- Boore D.M., Joyner W.B., Fumal T.E. Equations for Estimating Horizontal Response Spectra and Peak Acceleration from Western North American Earthquakes: A Summary of Recent Work. *Seism. Res. Let.* 1997; 68(1): 128-153.
- Cornell C.A. Engineering seismic risk analysis. *BSSA* 1968; 58: 1583-1606.
- Csomor D., Kiss Z. *Geofizikai Közlemények* 1959; 7: 169-180 (in Hungarian)
- Csontos L., Márton E., Wórum G., Benkovics L. Geodynamics of SW-Pannonian inselbergs (Mecsek and Villány Mts, SW Hungary): Inferences from a complex structural analysis. In *Neotectonics and surface processes: the Pannonian basin and Alpine/Carpathian system*, S. Cloetingh, F. Horváth, G. Bada, A. Lankreijer, eds., EGU St. Mueller Special Publication Series 2002; 3: 9-28.
- Deseő É., *Maximális talajvízállás (1961-1980) (térkép)*, 1:2 000 000, Magyarország Nemzeti Atlasza, MÁFI, Budapest, 1989.
- Dieterich J.H. A constitutive law for rate of earthquake production and its application of earthquake clustering. *J. Geophys. Res.* 1994; 99(2): 2601-2618.
- Fodor L., Csontos L., Bada G., Benkovics L., Gyórfi I. Tertiary tectonic evolution of the Carpatho-Pannonian region: a new synthesis of paleostress data. *Geol. Soc. Lond. Spec. Publ.* 1999; 156: 295-334.
- Gerner P., Bada G., Dövényi P., Müller B., Oncescu M.C., Cloetingh S., Horváth F. Recent tectonic stress and crustal deformation in and around the Pannonian basin data and

- models. In *The Mediterranean basins: Tertiary extension within the Alpine orogen*, B. Durand, L. Jolivet, F. Horváth, M. Séranne, eds., Geol. Soc. London Spec. Publ. 1999; 156: 269-294.
- Grenczy G., Fejes I., Kenyeres A. Present crustal deformation pattern in the Pancardi Region: Constraints from Space Geodesy. In *Neotectonics and surface processes: the Pannonian basin and Alpine/Carpathian system*, S. Cloetingh, F. Horváth, G. Bada, A. Lankreijer, eds., EGU St. Mueller Special Publication Series 2002; 3: 65-77.
- Grünthal G., Bosse C., Sellami S., Mayer-Rosa D., Giardini D. Compilation of the GSHAP regional seismic hazard for Europe, Africa and the Middle East. *Annali di Geofisica* 1999; 42(6): 1215-1223.
- Gutenberg J., Richter C.F. Frequency of earthquakes in California. *BSSA* 1944; 34: 185-188.
- Horváth F. Neotectonic behaviour of the Alpine-Mediterranean region. In *The Pannonian Basin - A study in basin evolution*, L.H. Royden, F. Horváth, eds., AAPG Memoir 1988; 45: 49-51.
- Horváth F., Cloetingh S. Stress-induced late-stage subsidence anomalies in the Pannonian basin. *Tectonophysics* 1996; 266: 287-300.
- Jámbor Á. Földtan (térkép), 1: 1 000 000, Magyarország Nemzeti Atlasza, MÁFI, Budapest, 1989.
- Karnik V. Seismicity of the European Area I. Praha, 1968.
- Lapajne J., Motnikar B.S., Zupancic P. Probabilistic Seismic Hazard Assessment Methodology for Distributed Seismicity. *BSSA* 2003; 93(6): 2502-2515.
- Lenkey L., Dövényi P., Horváth F., Cloetingh S.A.P.L. Geothermics of the Pannonian basin and its bearing on the neotectonics. In *Neotectonics and surface processes: the Pannonian basin and Alpine/Carpathian system*, S. Cloetingh, F. Horváth, G. Bada, A. Lankreijer, eds., EGU St. Mueller Special Publication Series 2002; 3: 29-40.
- Lew M. 2001. Liquefaction Evaluation Guidelines for Practicing Engineering and Geological Professionals and Regulators. *Environmental & Engineering Geoscience* 2001; VII(4): 301-320.
- Musson R. Probabilistic seismic hazard maps for the North Balkan region. *Annali di Geofisica*, 1999; 42(6): 1109-1124.
- Sadigh K., Chang C.-Y., Egan J.A., Makdisi F., Youngs R.R. Attenuation Relationships for Shallow Crustal Earthquakes Based on California Strong Motion Data. *Seism. Res. Lett.* 1997; 68(1): 180-189.
- Slejko D., Peruzza L., Rebez A. Seismic hazard maps of Italy. *Ann. Geophys.* 1998; 41: 183-214.
- Stein S., Newman A. Characteristic and Uncharacteristic Earthquakes as Possible Artifacts: Applications to the New Madrid and Wabash Seismic Zones. *Seismological Research Letters* 2004; 75(2): 173-187.
- Tóth L., Mónus P., Zsíros T. and Kiszely, M., Seismicity in the Pannonian Region – earthquake data. In *Neotectonics and surface processes: the Pannonian basin and Alpine/Carpathian system*, S. Cloetingh, F. Horváth, G. Bada, A. Lankreijer, eds., EGU St. Mueller Special Publication Series 2002; 3: 9-28.
- Tóth L., Mónus P., Zsíros T., Kiszely M. Micro-seismic monitoring of seismoactive areas in Hungary. *Studi Geologici Camerti*, Special Issue: Proceedings of the workshop COST Action 625 "Active faults: analysis, processes and monitoring" 2004.
- Zsíros T. Macro-seismic focal depth and intensity attenuation in the Carpathian region. *Acta Geod. Geoph. Hung.* 1996; 31:115-125.
- Zsíros T. A Kárpát-medence szeizmicitása és földrengés veszélyessége: Magyar földrengés katalógus (456-1995). MTA GGKI, Budapest 2000, ISBN 9638381159. p. 495 (in Hungarian).
- Zsíros T. Earthquake activity and hazard in the Carpathian basin I. *Acta Geod. Geoph. Hung.* 2003a; 38(3): 345-362.

Zsiros T. Earthquake activity and hazard in the Carpathian basin II. Acta Geod. Geoph. Hung.
2003b; 38(4): 445-465.